ELSEVIER

Thermochimica Acta 361 (2000) 31–52

thermochimica
acta

www.elsevier.com/locate/tca

The formation of Cu_2S from the elements
I. Copper used in form of powders

R. Blachnik*, A. Müller

Institute of Chemistry, University of Osnabrück, Barbarastr. 7, D-49069 Osnabrück, Germany

Received 2 December 1999; received in revised form 14 February 2000; accepted 16 February 2000

Abstract

The synthesis of Cu_2S from copper and sulfur from various sources has been studied in the DTA from 25 to 600°C. The educts and products were characterised by X-ray diffraction. Mixtures of copper and sulfur were investigated in form of powders and of pellets.

In the beginning of the reaction sulfides with high sulfur content are formed. In powders the main reaction takes place immediately after melting of sulfur whereas in pellets the larger exothermic effects appear at higher temperatures. In most samples the formation of Cu_2S is completed above 450°C. The difference in behaviour of powders and pellets is mainly based on the sample-crucible geometry, but also on different educt concentrations. Similar investigations were performed by mechanical alloying in a planetary ball mill with total milling times in the range 1–120 min. CuS, $Cu_{1.8}S$, $Cu_{1.95}S$, $Cu_{1.96}S$, and α-Cu_2S are formed in this order with increasing milling times. Almost no overlap in their formation was observed, because the brittle copper sulfides are removed by milling from the surface of the particles. The formation of further products is thus not hindered. Particle size, pretreatment and source of copper but not of sulfur influences significantly the reaction. The behaviour of copper powder of various manufacturers differed, despite the same pretreatment and particle size ranges, due to differences in particle size distribution, particle shape, grain size or oxygen content. Ageing experiments revealed that less metastable products are formed than in milling experiments or in quenched samples. Ageing in inert atmosphere produces CuS and does not exceed this stage even after several months. Different intermediate products were formed with a higher rate from the beginning, when the samples were stored in vacuum after short irradiation with intense light.

Keywords: Copper; Sulfur; Copper sulfide; Solid state reaction; Reactivity

---

1. Introduction

In the past many investigations dealt with the copper–sulfur system because of its importance in mineralogy and geology [1]. At least nine copper minerals have been identified [2,3]. During the last decades technological applications of copper sulfides were discovered. Some copper sulfides are p-type semiconductors [4]. α-Cu_2S is used in p-Cu_2S/n-CdS solar cells [4,5]. $Cu_{2-x}S$, a fast superionic conductor with structural disorder [6], is a promising material for thermo- and photoelectric transformers and high temperature thermistors [7]. CuS shows metallic conductivity and transforms at 1.6 K into a superconductor [8].

For these reasons thermodynamic data and phase equilibria of the copper sulfur system are well known.

---

* Corresponding author. Fax: +49-541-969-2370.
E-mail address: rblachni@rz.uni-osnabrueck.de (R. Blachnik).

PII: S0040-6031(00)00545-1

Less information is available for reaction pathways and conditions on which copper and sulfur react to sulfides. Some authors reported the formation of copper sulfides from the elements in aqueous or non-aqueous solutions [9–13]. Charbonnier and Murat [14] studied the synthesis of sulfides of groups 11 and 12 in the DTA in the range 25–1000°C with a heating rate of 2.5 K/min. The formation was indicated by one exothermic effect at 120°C for copper. The nature of the products obtained after cooling depended on the temperature at which they had been heated. Complete reaction was only observed for Cu_2S. Other authors used the high reactivity for synthesis of copper sulfides at rather low temperatures (200–350°C) [11,15,16]. Donnay et al. found that in Cu+S mixtures in the molar ratio of 9:5 the lowest reaction temperature was 25°C, but that the reaction was not complete after 5 months. At 90°C all copper has reacted to digenite in about 8 weeks (200°C, 2 weeks; 400°C, 2 days) [17]. However, these results are different from those of Djurle [18]. He found that pellets with different Cu:S ratios did not react completely within 1 week, even at 470°C. Moh reacted copper filings with sulfur in evacuated silica tubes. After 4 weeks at 50°C a non-equilibrium assemblage of grains with chalcocite in the centre and successive rings of digenite, blue-remaining covellite ($Cu_{1.1}S$), and covellite (CuS) was found [19,20]. Ohtani et al. [21] prepared two metastable copper sulfides and stable CuS by mechanical alloying in a planetary ball mill for 60 min. In the composition range $0.334<x_S<0.342$ ($Cu_{1.99}S$–$Cu_{1.92}S$) the tetragonal phase ($Cu_{1.96}S$) was obtained. Between $0.346<x_S<0.369$ ($Cu_{1.89}S$–$Cu_{1.71}S$) the reaction yielded a rhombohedral modification of low-digenite ($Cu_{1.8}S$). After ageing out of these metastable phases at room temperature, only the first one transforms sometimes to a stable phase.

In view of the lack of knowledge and of contradictory results on the reactivity we intended to investigate the factors which influence the formation of Cu_2S from the elements. Investigated parameters were amongst others shape of samples, mechanical treatment, pretreatment, particle size, and ageing. In all experiments only one parameter was changed to examine its influence on the DTA trace of a mixture of Cu and S. All intermediate and the final products were characterised by X-ray analyses.

2. Phase diagram and compounds

Chakrabarti and Laughlin [1] published in 1983 an assessed phase diagram (Fig. 1). The phase relations above 200°C had been previously verified by Sharma and Chang with thermodynamic calculation [23].

The copper–sulfur system is dominated by $Cu_{2-x}S$, high-digenite (Dg), which melts congruently at 1130°C. Large miscibility gaps exist on both sides of $Cu_{2-x}S$. At lower temperatures the broad homogeneity range is divided in several phase regions. These compounds are also found as minerals: $Cu_{1.75}S$ anilite (An), $Cu_{1.95}S$ djurleite (Dj), α-Cu_2S low-chalcocite (αCh) and β-Cu_2S high-chalcocite (βCh) (Table 1, Fig. 2). A stoichiometric compound CuS (Cv, covellite) decomposes peritectically at 507°C into $Cu_{2-x}S$ and liquid. The terminal solid solubility of sulfur in copper is very small, that of copper in sulfur is probably negligible [23]. The phase relations are complicated by a tendency to form metastable phases.

Within the homogeneity range of $Cu_{2-x}S$, α-Cu_2S or $Cu_{1.95}S$ and metastable $Cu_{1.96}S$ are found on cooling at higher copper contents [25]. The latter is also obtained by grinding. At lower copper contents metastable low-digenite, $Cu_{1.8}S$, is obtained from high-digenite on cooling. It is also known as mineral in several modifications due to its incommensurable structure [26–28]. Stable anilite transforms into a low-digenite modification on grinding [29]. In the literature it is controversial whether low-digenite is a stable [25,30] or a metastable phase [24,29]. We regard it as metastable in accordance with the phase diagram of Chakrabarti and Laughlin [22]. Some phase transformations are influenced by the thermomechanical history or show hysteresis [30–32].

3. Experimental

3.1. Methods

The thermal analyses were performed with a DTA device, developed by Gather [33] (thermocouples: Ni/CrNi; control unit: Novocontrol Newtronic Micro 96 TP5; recorder: Laumann Servokass 600). The system was calibrated with the melting points of gallium, indium, lead, antimony, and silver. The samples were

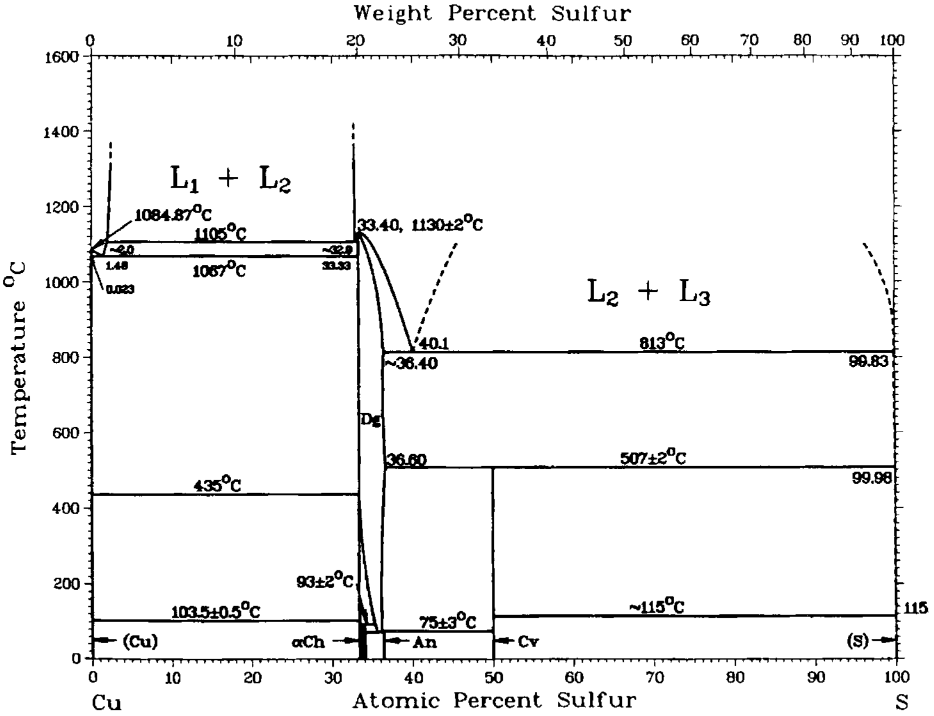

Fig. 1. Phase diagram of the system copper–sulfur [22].

Table 1
Stable and some metastable copper sulfides

Mineral or common name	Formulae used in the literature	Formula used in this work	Composition range y in Cu_yS [1]
High-temperature phases			
High-digenite	Cu_2S, γ-Cu_2S, α-Cu_2S, $Cu_{1.8}S$, $Cu_{2-\delta}S$, β-$Cu_{2-\delta}S$, $Cu_{2-x}S$	$Cu_{2-x}S$	2.002–1.732
High-chalcocite	Cu_2S, β-Cu_2S, β-$Cu_{2-\delta}S$	β-Cu_2S	2.000–1.988
Low-temperature phases			
Low-chalcocite	Cu_2S, α-Cu_2S, γ-Cu_2S, $Cu_{2-\delta}S$	α-Cu_2S	2.000–1.993
Djurleite	$Cu_{1.97}S$, α-$Cu_{1.97}S$, $Cu_{1.96}S$, $Cu_{1.95}S$, $Cu_{1.94}S$, $Cu_{1.938}S$, $Cu_{31}S_{16}$	$Cu_{1.95}S$	1.965–1.934
Anilite	$Cu_{1.75}S$, Cu_7S_4	$Cu_{1.75}S$	1.750
Covellite	CuS	CuS	1.000
Metastable phases			
Tetragonal phase	$Cu_{1.96}S$, $Cu_{2-\delta}S_{tetr}$	$Cu_{1.96}S$	2.00–1.95 (1.89); 1.99–1.92 [21][a]
Low-digenite[b]	α-$Cu_{2-\delta}S$, $Cu_{1.8}S$, $Cu_{1.81}S$, $Cu_{7.2}S_4$, Cu_9S_5, $Cu_{9+x}S_5$, $Cu_{9-x}S_5$, Cu_7S_4	$Cu_{1.8}S$	1.83–1.77 [24]; 1.89–1.71 [21][a]
Roxbyite[b]	$Cu_{1.74-1.82}S$, Cu_7S_4	$Cu_{1.75}S$	1.82–1.74 [3]
Blue-remaining covellite, yarrowite	$Cu_{1.1}S$, Cu_9S_8, $Cu_{1+x}S$	$Cu_{1.1}S$	1.0–1.2 [24]; 1.1–1.2 [20]

[a] In mechanochemical synthesis.

[b] In nature stabilised by traces of iron.

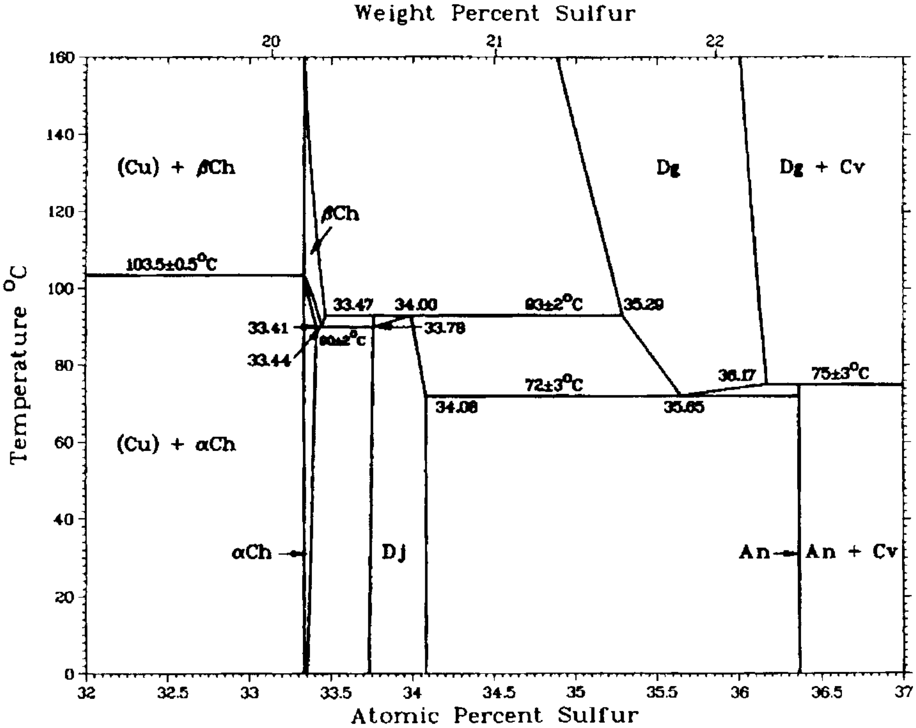

Fig. 2. The homogeneity range of $Cu_{2-x}S$ at low temperatures [22].

sealed in evacuated silica ampoules (length: 3.5 cm; diameter: 4.0 mm; wall thickness: 0.5 mm; Fig. 3a and b). The runs were done with a heating rate of 10 K/min, a sample mass of 0.12–0.18 g, silicon as reference, and in the range 25–600°C.

In some cases a DSC 404C Pegasus (Netzsch; high temperature furnace; DSC sensor with chromel–constantan thermocouples) was used and calibrated as described, but silver was substituted by zinc. The samples with a mass of about 100 mg were measured in evacuated and sealed silica crucibles (length: 1.5 cm; diameter: 6.3 mm; wall thickness: 0.4 mm; Fig. 3c) in the temperature range 25–550°C. An empty silica crucible served as reference. The temperatures of effects were determined from the onset of the peaks.

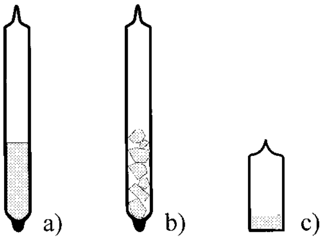

Fig. 3. Arrangement of samples. (a) Powder (DTA); (b) fragmented pellet (DTA) and (c) pellet (DSC).

X-ray measurements were carried out with the aid of a transmission powder diffractometer STADI P (Stoe), using Cu Kα1 radiation (154.051 pm), a germanium single crystal monochromator, and a linear position sensitive detector. Temperature dependent X-ray measurements were performed with a high temperature attachment. Transmission diffractograms were started at 70°C and ended at 390°C in 10°C steps. After heating in 10 min to the next temperature followed an equilibration period of 15 min. In some cases, at room temperature, a Huber Vertical Guinier Camera 620 and at high temperatures an Enraf Nonius Guinier Simon Camera FR 553 (heating rate: 0.17 K/min) were used. For the high temperature measurements the samples were placed in evacuated and sealed silica capillaries. X-ray measurements were interpreted by comparison with the PDF-2 database of JCPDS-International Centre for Diffraction Data [34] or by simulation of XRD patterns with single crystal data from ICSD [35]. Both procedures were performed with the program VISUAL X^{POW} [36].

Microscopical investigations were done with a microscope (Olympus) with a maximum magnification of forty. Scanning electron microscope pictures were taken with a DMS 962 (Zeiss).

3.2. Chemicals

Table 2 contains the sources and some properties of the different batches of copper and sulfur, used in the studies.

For desoxidation copper was placed in a silica tube. A mixture of 90% N_2 and 10% H_2 was passed over the sample for 4 h (0.5 h at 260°C). Copper powders with defined particle sizes were produced with an analytical sieve shaker (AS 200 basic, Retsch). Sulfur was either sublimed in an evacuated glass tube in a temperature gradient from 100°C to room temperature over a period of 6 weeks or recrystallised twice from CS_2. After the latter procedure the product was treated in vacuum at 150°C for 0.5 h to remove solvent and traces of water. After purification the elements were stored under argon.

If not otherwise mentioned, recrystallised sulfur (Merck) and copper powders (Heraeus) with a particle size range 36–100 μm reduced at 550°C were used as educts. In high-temperature X-ray measurements copper powders (Guinier Simon camera: Heraeus, particle size 36–100 μm; transmission diffractometer: Heraeus, particle size 32–36 μm) were used after reducing at 260°C.

3.3. Preparation and measurement

Samples with the stoichiometry of Cu_2S were obtained by weighing corresponding amounts of the elements (accuracy ± 1.0 mg) and mixing in an agate mortar. Some of these mixtures were characterised by X-ray diffraction prior to heating. Pellets for the DTA (DSC) with a diameter of 6.0 mm (5.0 mm) were pressed from these mixtures with a pressure of 0.69 GPa (0.75 GPa). Pellets for the DTA were broken into smaller pieces.

Quartz ampoules were heated in vacuum to remove water, flushed with argon, and then filled. During sealing the end of the ampoule was cooled to prevent reaction. Immediately after sealing the samples were used for thermal analyses to avoid ageing effects. Most samples contained copper after the DTA runs, due to loss of sulfur in all steps of the preparation, but especially during grinding. This effect increases with the size of copper particles and could not be compensated by a slight excess of sulfur.

Thermal effects were characterised with ex situ X-ray measurements by quenching samples from the

Table 2
Copper and sulfur studied in this investigation

Element	Source	Shape	Purity[a] (%)	Purification methods	Particle size[b] (μm)
Copper	ABCR	Shot	99.999	–	–
Copper	Alfa	Shot	99.999	–	–
Copper	Alfa	Powder	99	Reduced at 500°C	<1
Copper	Alfa	Tinsel	99.5	Reduced at 550°C	<45
Copper	Goodfellow	Foil	OFHC[c], 99.95	Reduced in ethanol or cleaned in HCl	Ø 500
Copper	Goodfellow	Powder	99.8	Reduced at 550°C	<500
Copper	Heraeus	Powder	99.8	Reduced at 260, 550, 600, 650°C	<100
Copper	Strem	Powder	99.999	Reduced at 550°C	<150
Copper	Strem	Powder	99.999	Reduced at 550°C	<150
Sulfur	Fluka	Powder	–	Sublimed, recrystallised	–
Sulfur	Merck	Powder	–	Sublimed, recrystallised	–
Sulfur	Riedel	Powder	99.5	Sublimed, recrystallised	–
Sulfur	Strem	Platelets	99.999	–	–

[a] For copper only metallic impurities.

[b] Given by producer.

[c] Oxygen-free high conductivity.

temperatures of the peak onset, the maximum and the end of the effect in ice–water mixture.

Two arrangements of educts which differ in density, concentration, and contact area are shown in Fig. 3. Different densities were achieved by using powders (Fig. 3a) or pellets (Fig. 3b). The density of pellets was $D=5.4$ g/cm^3, powders $D=2.7$ g/cm^3 and that of compact α-Cu_2S $D=5.7$ g/cm^3 [37]. By dilution of the reaction mixtures with SiO_2 the concentration of educts and the contact area were varied within the same geometry. In these experiments the educts were carefully blended with silica powder in a mass ratio 1:1 with a spatula. Product concentrations were calculated from densities and were in powders $c=17$ mol/l, in pellets $c=35$ mol/l, and in pellets of diluted mixtures $c=9$ mol/l.

Mechanical alloying was performed with a planetary ball mill (Pulverisette 7, Fritsch) with hardmetal tungsten carbide bowls ($V=12$ ml) and milling balls (Ø 12 cm) in argon. The rotational speed was 400 rpm and the mass of samples approximately 4 g. The mill was stopped in intervals and parts of the powder mixture were investigated.

In ageing experiments of powders one part of samples was stored under argon, another in evacuated quartz ampoules at room temperature. The mixtures were shaken every second day.

The influence of heating rates on the formation of Cu_2S in pellets was investigated using a DSC 404 with heating rates of 1.0, 2.5, 5.0, 10, 20, and 40 K/min.

4. Results and discussion

4.1. Characterisation of copper and sulfur

In Tables 3 and 4 as received and purified sulfur and copper samples from various sources are characterised.

Pure copper melts at 1084.6°C. In the DTA traces of the different copper charges up to three effects were found. A typical melting peak was observed with oxygen free copper foils. Oxygen is dissolved in the liquid metal during the production process, and appears after solidification at the grain boundaries as Cu_2O [38,39]. Thus, the Cu–Cu_2O eutectic

Table 3
Appearance, oxygen content and thermal data of purified and unpurified copper

Copper	Appearance	Appearance after melting	XRD pattern[a]	Thermal effects, t (°C)
ABCR, shot, unpurified	Copper coloured	Light pink	Cu	1062, 1072
Alfa, shot, unpurified	Copper coloured	–	Cu	1062, 1077, 1086
Alfa, powder, unpurified	Black	–	Cu, CuO, Cu_2O	1019, 1070, 1093
Alfa, powder, purified	Violet	Light pink-black	Cu, Cu_2O[b]	1056, 1061
Alfa, tinsel, unpurified	Copper coloured	Light pink-black	Cu, Cu_2O[b]	1075[c], 1081
Alfa, tinsel, purified	Pink	Light pink-black	Cu, Cu_2O[b]	1073, 1082
Goodfellow, foil, unpurified	Copper coloured	Light pink	Cu	1078
Goodfellow, foil, purified	Light pink	Light pink	–	1081
Goodfellow, powder, unpurified	Copper coloured	Light pink	Cu	1073, 1083
Goodfellow, powder, purified	Light pink	Light pink	Cu	1074, 1082
Heraeus, powder, unpurified	Brown	Dark red-brown	Cu, Cu_2O	1058
Heraeus, powder, reduced at 260 °C	Light pink	Dark red-brown	Cu, Cu_2O	1061, 1066
Heraeus, powder, reduced at 550 °C	Light pink	Light pink	Cu	1059, 1069, 1072
Heraeus, powder, reduced at 650 °C	Light pink	Light pink	Cu	1068, 1075
Strem, powder, unpurified	Black-violet	–	Cu, CuO[b]	–
Strem, powder, purified	Copper coloured	Light pink-copper coloured	Cu	1057, 1064
Strem, powder, unpurified	Copper coloured	Light pink	Cu	1059, 1064
Strem, powder, purified	Copper coloured	Light pink	Cu	1062, 1073, 1084

[a] By powder diffractometry Cu_2O contents determined down to a mole fraction of $x_0=0.001$.

[b] Very low concentration.

[c] Exothermic thermal effect.

Table 4
Appearance and thermal data of purified and unpurified sulfur

Sulfur	Appearance	Appearance after melting	XRD pattern	Thermal effects, t (°C)
Fluka, unpurified	Yellow	Grey yellow	α-S_8	108, 121, 172
Fluka, sublimed	Yellow crystals	Brown	α-S_8	114, 122, 175
Fluka, recrystallised	Yellow	Yellow	α-S_8	105, 120, 189
Merck, unpurified	Yellow	Grey brown	α-S_8	104, 121, 174
Merck, sublimed	Yellow crystals	Ocher yellow	α-S_8	110, 123, 184
Merck, recrystallised	Yellow	Yellow	α-S_8	102, 120, 177
Riedel, unpurified	Yellow	Dark yellow	α-S_8	106, 119, 174
Riedel, sublimed	Yellow crystals	Light brown	α-S_8	113, 122, 180
Riedel, recrystallised	Yellow	Yellow	α-S_8	105, 120, 183
Strem, unpurified	Yellow	Yellow	α-S_8	106, 120, 171

(x_0=0.017, t=1066°C) was found in thermal analyses. Although preparation procedures suggest for the reduction of copper oxides with hydrogen a temperature range 175–300°C [40,41], we found that at 260°C only surface layers were removed. All oxides were reduced above 500°C.

The SEM pictures in Fig. 4 show the different shapes of powders obtained from various sources and production processes. Fig. 4c and d reveal the very high specific surface area of these particles (alfa). The thickness of the platelets can be estimated to 250 nm. Comparison between Fig. 4e and f gives evidence of hydrogen embrittlement. The cracks were caused from water vapour which is deposited at grain boundaries during reduction of Cu_2O with hydrogen. This occurs generally above 450°C [38,39].

The DTA traces of sulfur reveal the transition α- to β-S_8, melting and polymerisation to ω-S. The temperatures of the first and the third effect depend on the heating rate [42]. The sulfur charges were classified into three groups (Table 5) by purification methods, of which the data of recrystallised sulfur agree well with the literature. However, its yellow colour indicated traces of S_7 [46].

4.2. Reproducibility

Several series of experiments were performed to ensure that differences in the reaction products and temperatures are due to altered parameters.

Three series of samples in the form of powders and pellets, each with at least four charges of the same educt mixture, were investigated under identical experimental conditions. DTA traces of powders were nearly identical whereas in those of pellets small peaks and shoulders were not reproducible and large thermal effects were separated, overlapped, or appeared as shoulders. These discrepancies increased at higher temperatures, especially the phase transition β-$Cu_2S \rightarrow Cu_{2-x}S$ was found sporadically. The average standard deviations of reaction temperatures (phase

Table 5
Thermal effects of sulfur before and after purification and literature data

Purification method	Phase transition point (°C)	Melting point (°C)	Polymerisation point (°C)
No purification	106	120	173
Sublimation	112	122	180
Recrystallisation	104	120	183
Heating rate 10 K/min	103[a] [43]	120 [42]	183 [42]
Heating rate extrapolated to 0 K/min	95 [44]	120 [44]	159 [45]

[a] Heating rate 5 K/min.

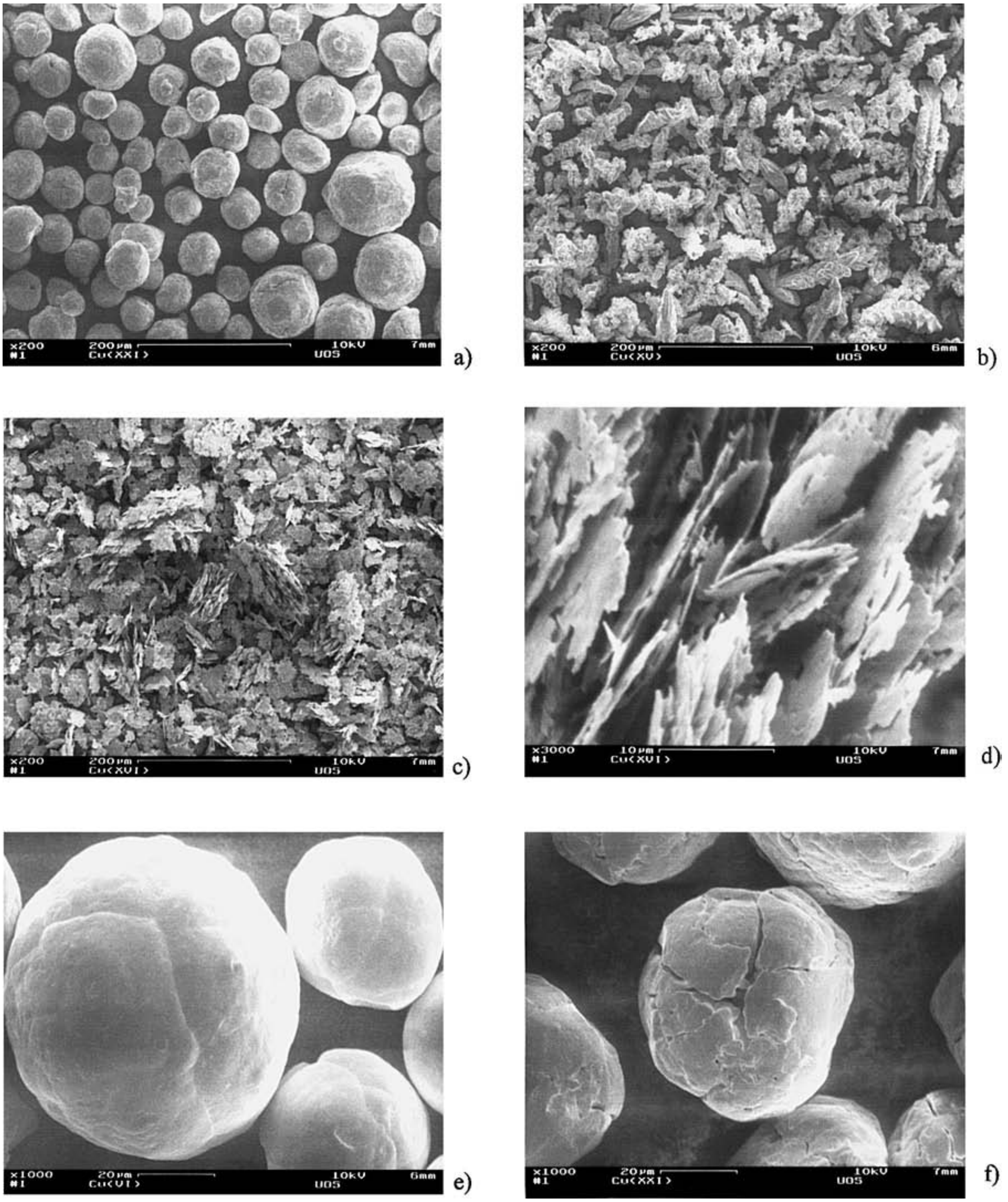

Fig. 4. SEM pictures of different copper powders. Particle size ranges were prepared with a sieve shaker. Magnification and scale at the bottom of each picture. (a) Heraeus, powder, reduced at 550°C, particle size 36–100 µm; (b) Goodfellow, powder, reduced at 550°C, particle size <32 µm; (c) alfa, tinsel, reduced at 550°C, particle size <32 µm; (d) 15 times magnification of a part of picture 'c', (e) Heraeus, powder, reduced at 260°C, particle size 36–100 µm and (f) five times magnification of a part of picture 'a'.

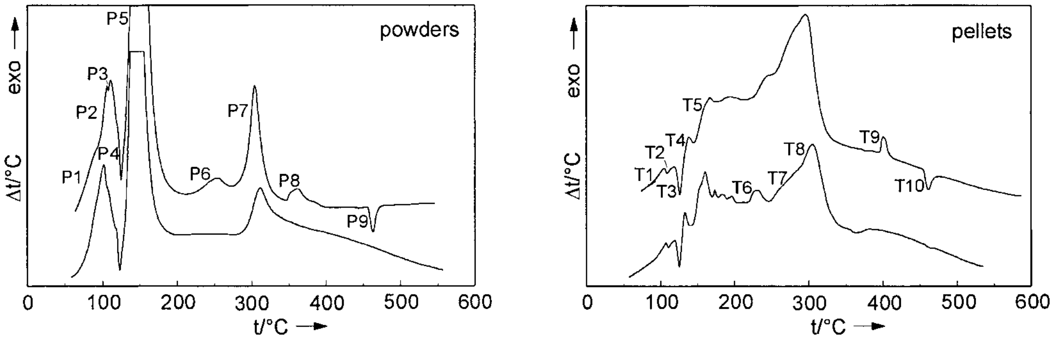

Fig. 5. Extremely varying DTA traces of different mixtures (2Cu+S) examined under identical conditions.

transition temperatures) are for powders ±3.5°C (±0.7°C) and for pellets ±3.4°C (±1.2°C). The moderate reproducibility of the shape of the effects is not indicated by these standard deviations.

Samples from different educt mixtures were investigated under identical conditions to judge the influence of inaccuracy of weighing, differences in homogeneity by different periods and pressures of mortaring, pellet production and ageing. For this reason four samples, each in the form of powders and pellets were compared. Extremely different DTA traces are presented in Fig. 5. The variances of effects in powders are now similar to those of pellets described above. The average values of the standard deviations of the onset temperatures of reactions (phase transitions) were for powders ±10.6°C (±1.3°C) and pellets ±9.1°C (±1.0°C). The reproducibility for samples of different charges was, thus, worse than for those of the same charge. In Fig. 6 the standard deviation is given with respect to onset temperatures. The maximums are found for powders and pellets at the highest temperatures.

4.3. Analyses of DTA traces

In this paragraph the course of the reaction in powders is described and can be followed with the aid of the phase diagram (Fig. 7). Marking of peaks can be taken from Fig. 5. Tables 6 and 7 contain the onset temperatures, Tables 8 and 9 the phases found in quenched mixtures. Reaction equations are summarised in Table 10.

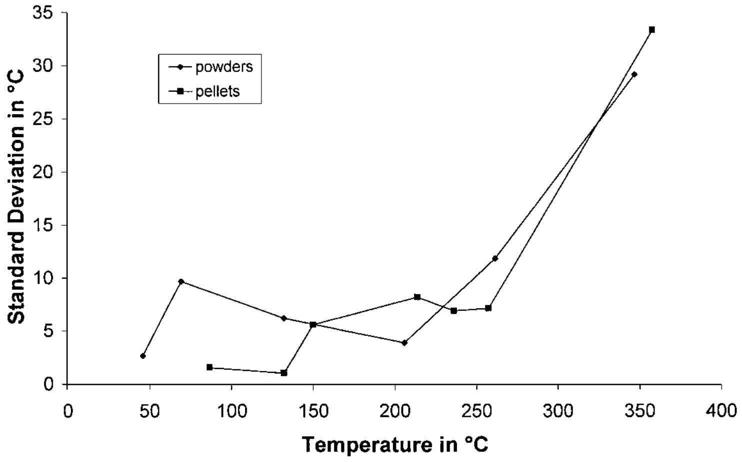

Fig. 6. Average values of the standard deviations of the onset temperatures of reactions.

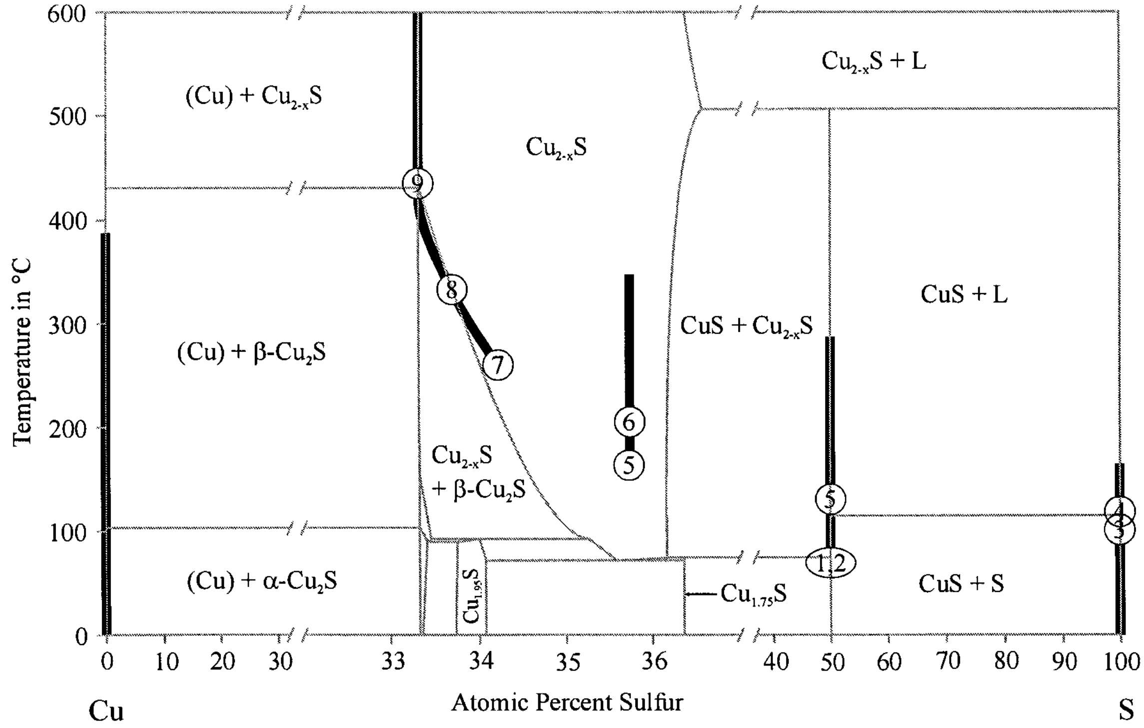

Fig. 7. Temperature ranges of phases and compounds during reactions in powders of (2Cu+S) according to the Cu–S phase diagram [22].

Educts turn to grey during mortaring by the formation of CuS. On heating further reaction to CuS starts at 46°C (P1) and increases at 70°C (P2). In these exothermic effects the reaction is restricted to the surface of the particles. The phase transformation of sulfur (P3) occurs within P2. The decaying flank of P2 is overlapped by the melting effect of sulfur (P4). In the next large exothermic peak (maximum at approximately 165°C, P5) all sulfur reacts to CuS. The samples consist now of deep blue-black balls with a core of copper. The compounds which are observed after quenching are given in brackets. The negligible amount of $Cu_{2-x}S$ ($Cu_{1.8}S$) observed from the beginning of the reaction (P1) does not increase in this

Table 6
Thermal effects of powders (2Cu+S)

Effect	P1	P2	P3	P4	P5	P6	P7	P8	P9
	Exo	Exo	Endo	Endo	Exo	Exo	Exo	Exo	Endo
t (°C)	46±3	70±10	102±1	119±2	132±6	206±4	262±12	348±29	450±1

Table 7
Thermal effects of pellets (2Cu+S)

Effect	T1	T2	T3	T4	T5	T6	T7	T8	T9	T10
	Exo	Endo	Endo	Exo	Exo	Exo	Exo	Exo	Exo	Endo
t (°C)	87±2	103±0	121±1	132±1	150±6	214±8	236±7	258±7	358±33	450±1

Table 8
Phases in quenched powders

Interruption of the reaction	Phases[a]
After grinding, before heating	Cu, α-S_8 [47], CuS [48][b]
During P2	Cu, α-S_8, CuS, $Cu_{1.8}S$ [49][b]
After P4	Cu, CuS, α-S_8, $Cu_{1.8}S$[b]
During P5	Cu, CuS, $Cu_{1.8}S$[b], α-S_8[b]
After P5	Cu, CuS, $Cu_{1.8}S$ [50][c]
Between P5 and P6	Cu, $Cu_{1.8}S$, CuS, $Cu_{1.95}S$ [51][b]
Before P7	$Cu_{1.8}S$, Cu, CuS, $Cu_{1.95}S$[b]
During P7	Cu, $Cu_{1.96}S$ [52], $Cu_{1.95}S$, $Cu_{1.8}S$, CuS[b]
After P7	$Cu_{1.96}S$, Cu, $Cu_{1.95}S$, $Cu_{1.8}S$
After P7	$Cu_{1.96}S$, Cu, $Cu_{1.95}S$, $Cu_{1.8}S$
After P7	$Cu_{1.96}S$, α-Cu_2S [53], Cu, $Cu_{1.95}S$
After cooling	α-Cu_2S, Cu

[a] Phases in order of intensities of reflections.
[b] Very low concentration.
[c] In other mixtures always low-digenite [49] was observed.

period. When P5 is declining CuS reacts slowly with Cu to sulfur rich $Cu_{2-x}S$. Proceeding reaction to $Cu_{2-x}S$ is indicated by two effects (P6, P7). During the first one, mostly a shoulder of P7, sulfur rich $Cu_{2-x}S$ ($Cu_{1.8}S$) is formed. The second indicates the appearance of copper rich $Cu_{2-x}S$ ($Cu_{1.95}S$, $Cu_{1.96}S$), by which CuS is consumed and the amount of sulfur rich $Cu_{2-x}S$ ($Cu_{1.8}S$) decreases. The samples consist now of coagulated, grey hollow spheres, which sometimes have brown-red copper cores. Blue-black particles are only observed in areas with direct contact to the atmosphere of the ampoule.

Table 9
Phases in quenched pellets

Interruption of the reaction	Phases[a]
After pressing, before heating	Cu, α-S_8, CuS[b]
After T3	Cu, α-S_8, CuS, $Cu_{1.8}S$[b]
During T5	Cu, CuS, $Cu_{1.8}S$[b], α-S_8[b,c]
After T5	Cu, CuS, $Cu_{1.8}S$[b], α-S_8[b,c]
During T6	Cu, CuS, $Cu_{1.8}S$[c]
After T6	Cu, CuS, $Cu_{1.8}S$, $Cu_{1.95}S$[b,c]
During T8	Cu, $Cu_{1.8}S$, $Cu_{1.95}S$, CuS
After T8	$Cu_{1.96}S$, Cu, $Cu_{1.8}S$, $Cu_{1.95}S$, CuS[b]
After T8	α-Cu_2S, $Cu_{1.96}S$, Cu
After T8	α-Cu_2S, Cu
After T8	α-Cu_2S, Cu
After cooling	α-Cu_2S, Cu

[a] Phases in order of intensities of reflections.
[b] Very low concentration.
[c] Amorphous sulfur was visible.

Table 10
Reactions during heating in powders (P) and pellets (T)

$$\mathrm{Cu} + \mathrm{S} \xrightarrow{\text{grinding, pressing}} \mathrm{CuS}$$

$$\mathrm{Cu} + \mathrm{S} \xrightarrow{\mathrm{P1,\ P2,\ T1}} \mathrm{CuS}$$

$$\alpha\text{-}\mathrm{S_8} \xrightarrow{\mathrm{P3,\ T2}} \beta\text{-}\mathrm{S_8}$$

$$\beta\text{-}\mathrm{S_8} \xrightarrow{\mathrm{P4,\ T3}} \mathrm{S_8(l)}$$

$$\mathrm{Cu} + \mathrm{S} \xrightarrow{\mathrm{P5,\ T4,\ T5,\ T6}} \mathrm{CuS}$$

$$\mathrm{CuS} + 1 - x\mathrm{Cu} \xrightarrow{\mathrm{P5,\ P6,\ T6,\ T7}} \mathrm{Cu}_{2-x}\mathrm{S}(x \approx 0.2)$$

$$\approx 1.8\mathrm{Cu} + \mathrm{S} \xrightarrow{\mathrm{T7}} \mathrm{Cu}_{2-x}\mathrm{S}(x \approx 0.2)$$

$$\mathrm{CuS} + 1 - x\mathrm{Cu} \xrightarrow{\mathrm{P7,\ T8}} \mathrm{Cu}_{2-x}\mathrm{S}(x \approx 0.05)$$

$$\mathrm{Cu}_{2-x}\mathrm{S}(x \approx 0.2) + \approx 0.15\mathrm{Cu} \xrightarrow{\mathrm{P7,\ P8,\ T8,\ T9}} \mathrm{Cu}_{2-x}\mathrm{S}(x \approx 0.05)$$

$$\mathrm{Cu}_{2-x}\mathrm{S}(x \approx 0.05) \xrightarrow{\mathrm{P8,\ T9}} [\mathrm{Cu}_{2-x}\mathrm{S}]'(x \approx 0.05) + \beta\text{-}\mathrm{Cu_2S}$$

$$\mathrm{Cu}_{2-x}\mathrm{S}(x \approx 0.05) + x\mathrm{Cu} \xrightarrow{\text{no}} \mathrm{Cu}_{2-x}\mathrm{S}(x = 0)$$

$$\beta\text{-}\mathrm{Cu_2S} \xrightarrow{\mathrm{P9,\ T10}} \mathrm{Cu}_{2-x}\mathrm{S}(x = 0)$$

The formation of Cu_2S is slow after P7 in most samples. No further thermal effect is observed, as given in Table 8. The effects P8 and P9 appear only at higher reaction rates. P8 indicates the formation of copper rich $Cu_{2-x}S$ from copper and rests of sulfur rich $Cu_{2-x}S$. In this case the mixtures pass from the homogeneity range of $Cu_{2-x}S$ into the two-phase region $Cu_{2-x}S$+β-Cu_2S, which leads to an additional exothermic contribution to P8. After this effect the transition β-$Cu_2S \rightarrow Cu_{2-x}S$ (x=0) is always observed. The reaction of copper and copper rich $Cu_{2-x}S$ to the stoichiometric composition causes no thermal effect.

The onset temperature of P9 (β-$Cu_2S \rightarrow Cu_{2-x}S$ (x=0)) of 450°C occurs in the broad temperature range reported for this transition [25,54]. Coagulated large, grey, and hollow spheres are observed after cooling.

The same course of the reaction was observed in the high temperature X-ray investigations (Fig. 8), though copper powders in the educts were finer and contained traces of oxygen. Similar to the observation with DTA β-Cu_2S [55] is not always observed.

Samples in form of pellets were black-grey because CuS was formed during grinding and pressing. The course of the reaction on heating is similar to that in powders. The CuS formation starts at 87°C (T1) and decays gradually. During this effect the phase transition α- to β-S_8 is observed (T2). In the declining T1

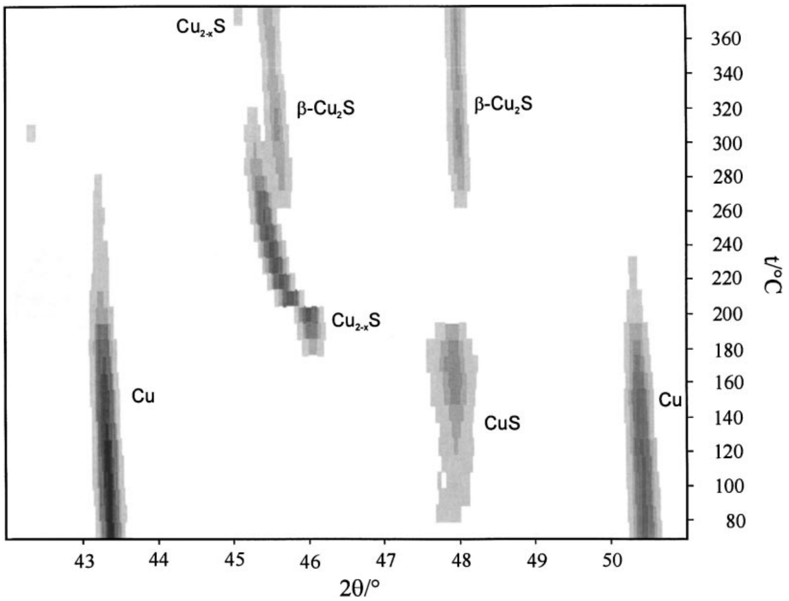

Fig. 8. Temperature dependent X-ray diffractograms of (2Cu+S) in Guinier presentation.

effect sulfur melts (T3) immediately followed by a weak exothermic effect (T4) and a stronger one at 150°C (T5). During these events CuS and some sulfur rich $Cu_{2-x}S$ ($Cu_{1.8}S$) are formed. At approximately 180°C most sulfur accumulates in the space between the pieces of the pellet, which consists now of copper particles surrounded by a dense black layer. The next thermal effects are overlapping. At T6 remaining sulfur in the pellets reacts to CuS, sulfur rich $Cu_{2-x}S$ ($Cu_{1.8}S$) is also formed. Rests of sulfur remain outside of the pellet. The effect at T8 and the shoulder at T7 are due to the reaction of CuS and this sulfur with copper to sulfur rich $Cu_{2-x}S$ and at higher temperatures to copper rich $Cu_{2-x}S$ ($Cu_{1.96}S$, $Cu_{1.95}S$). On further heating no difference is observed to powdered samples.

The appearance of effects in DTA curves is determined by the shape of the samples. Pellets give DTA traces with strongly overlapping effects. Powders react mainly after melting of sulfur. In pellets the thermal effects at lower temperatures are smaller compared with powders. Strong exothermic effects appear at higher temperatures when sulfur evaporates. In both cases the reaction ends at approximately the same temperature (P7, T8). The contact area between copper and sulfur is significantly higher in pellets than in powders due to the higher density and resulting higher educt concentration. However, the differences in reaction behaviour of powders and pellets were based on the different sample-crucible geometry, i.e. the empty space between the individual pieces of the pellets or between pellet and crucible walls. Thicker layers of CuS build up during the production of the pellets. These layers protect copper against reaction at low temperatures, which begins therefore at higher temperatures and is hindered even after melting of sulfur. Thus, liquid sulfur flows into the space between the pellets and cannot take part in the reaction before partial evaporation.

No difference was observed in reactions of undiluted and with SiO_2 diluted powders within reproducibility. Diluted pellets reveal striking differences in DTA curves compared with those of undiluted samples. Effects immediately before and after melting of sulfur are more intense, the following thermal effects have approximately the same intensity and are well separated except T7 and T8. The results confirm that differences between powders and pellets are caused by different sample-crucible geometries as well as by different educt concentrations.

4.4. *Influence of mechanical treatment*

Difference in mechanical treatment could be achieved by mixing powders with a spatula, by variation of the pressure during pellet fabrication, or by variation of milling times in the planetary ball mill.

4.4.1. *Mixing with a spatula*

Prior to produce the reaction mixture sulfur and copper powder had to be ground in an agate mortar. To minimise the influence of mortaring at first sulfur was mortared and then carefully blended with copper powder by stirring with a spatula. The effects P1, P2, and P5 merge now in DTA runs to one strong exothermic peak prior to the melting of sulfur. The reaction rate increases vehemently revealed by a suddenly steep increase of the sample temperature. The mixtures are much more reactive because a protecting CuS layer is not formed.

4.4.2. *Influence of pressure*

Reaction mixtures were subjected immediately after mortaring to pressure (0.12, 0.25, 0.50, 1.00, 1.38 GPa) for 1 min and then investigated by X-ray diffractometry. The formation of CuS increases with increasing pressures. The intensity ratio of CuS versus Cu reflections grew for example by a factor three when the mixture was treated for 1 min with 1.38 GPa, compared with an untreated sample.

4.4.3. *Influence of milling time*

The total milling times were in the range 1–120 min. Fig. 9 shows diffractograms and DTA traces of samples. Milled samples were investigated twice in form of pellets in the DTA. In the first stage of the syntheses the amount of CuS increases until after 20 min all sulfur is consumed. The DTA traces show after short milling (1–2 min) a better separation of effects which is accompanied by larger areas of peaks in the lower temperature range (T4, T5), compared with those of untreated samples. After 5 min the DTA trace is very similar to those of powders. The main reaction occurs now directly after the melting of sulfur. After longer milling periods (20 min) the CuS reaction and the melting effect of sulfur vanish. In the next milling step Cu reacts with CuS to metastable low-digenite ($Cu_{1.8}S$, 40 min) [49]. Hence, the thermal effect (T11), which indicate the formation of sulfur rich $Cu_{2-x}S$ become smaller. The effect T9 which simultaneously increases in sharpness is due to the reaction of sulfur rich to more copper rich copper(I) sulfide. After 40 min at first djurleite ($Cu_{1.95}S$) and then metastable $Cu_{1.96}S$ is observed in the diffractograms. In the DTA an endothermic effect at 95°C indicates the peritectoid decomposition of djurleite. The onset temperature of the formation of copper rich $Cu_{2-x}S$ (T9) is shifted by ca. 100°C to lower temperatures. After 80 min α-Cu_2S appears and coexists with $Cu_{1.96}S$ until the complete consumption of Cu after 120 min. In the respective DTA traces the decomposition effects of djurleite disappear. The phase transition α- to β-Cu_2S is observed only after 80 min milling at 104°C, then it vanishes. Parallel to that the superstructure X-ray reflections of α-Cu_2S are broad and very weak due to mechanical treatment [32]. Remarkable is the observation of the gradual shift of the β-Cu_2S to $Cu_{2-x}S$ ($x=0$) transition from 450 to 480°C with increasing milling times. After milling periods over 80 min the samples contain WC [56] of the milling balls.

Intensity and sharpness of the first reaction effects increase with milling times so that overlapping DTA effects separate completely. With increasing milling times peak after peak disappears. With the exception of T9 all onset temperatures do not change significantly. The reproducibility of DTA curves increases considerably after 5 min milling, sporadic small effects and shoulders typically for pellets vanish.

Intermediate products are well reproducible after equal milling intervals. Some metastable and all stable copper sulfides are observed, except anilite ($Cu_{1.75}S$) because it transforms rapidly to low-digenite already by mortaring. The copper content of the compounds increases with milling time and almost no overlap in their formation was observed (Table 11). The reason for this effect may be that the brittle copper sulfides are removed by milling from the surface of the ductile particles so that the formation of kinetically favoured products is not hindered by a product layer.

Similar investigations of Ohtani et al. [21] are not comparable because they milled in each case for 60 min and identified at the respective educt compositions $Cu_{1.96}S$, $Cu_{1.8}S$, and CuS but never $Cu_{1.95}S$. In the copper rich region they obtained up to the composition of $Cu_{1.99}S$ only $Cu_{1.96}S$.

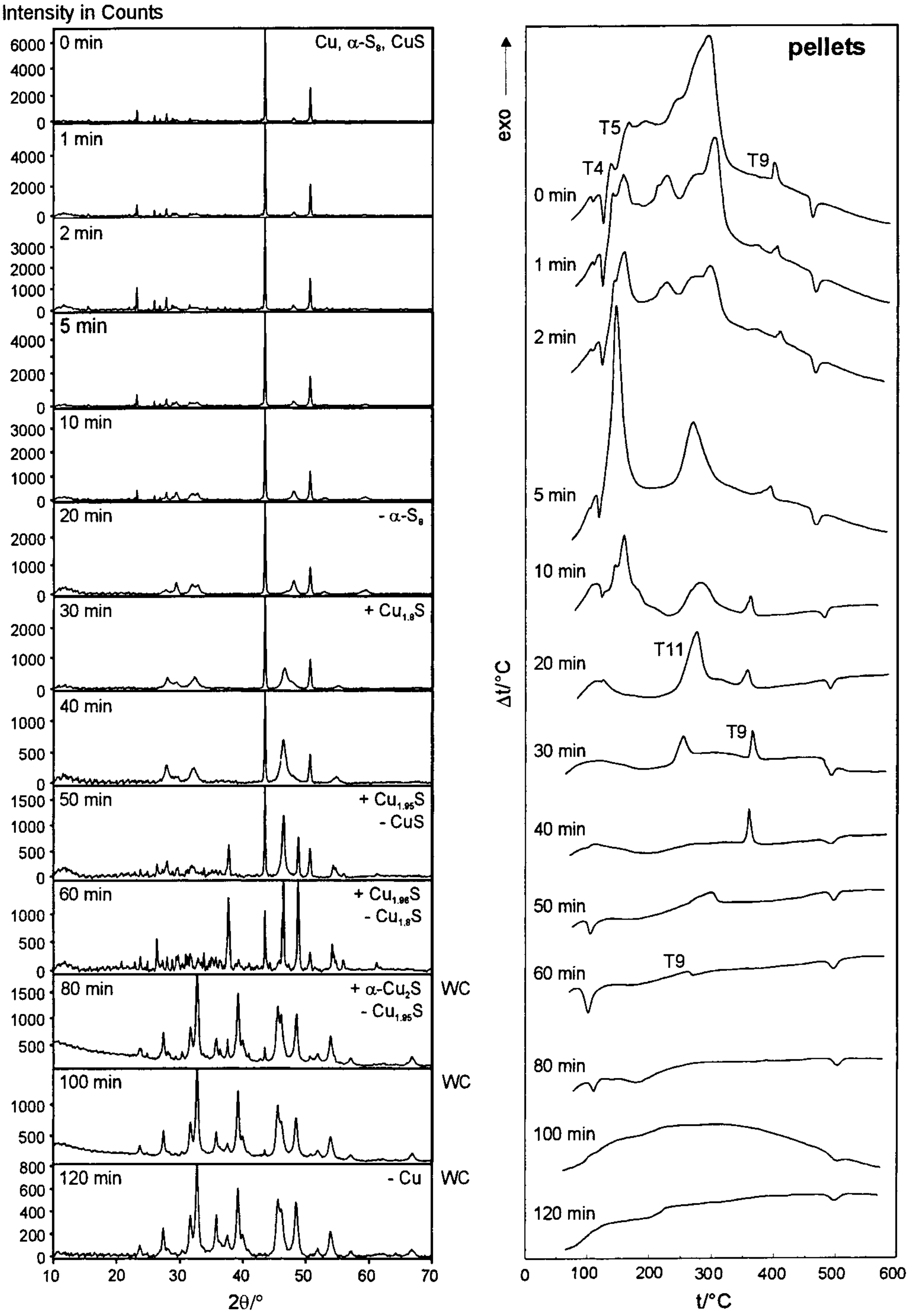

Fig. 9. XRD patterns before DTA run and belonging DTA traces of samples with different total milling time.

Table 11
Reactions during milling

$Cu + S \rightarrow CuS$
$CuS + 0.8Cu \rightarrow Cu_{1.8}S$
$Cu_{1.8}S + 0.15Cu \rightarrow Cu_{1.95}S$
$Cu_{1.95}S + 0.01Cu \rightarrow Cu_{1.96}S$
$Cu_{1.95}S + 0.05Cu \rightarrow \alpha\text{-}Cu_2S$

4.5. Influence of the particle size of copper

The influence of particle size was investigated with sieved and reduced copper powders (Heraeus) with particle diameter ranges of 100–112μm (I), reduced at 600°C, 36–100 μm (II), and <32 μm (III) both reduced at 550°C. In Fig. 10 the DTA traces for powders and pellets are shown.

The DTA curves with copper powders of range I and II are similar, only the reaction peaks are better separated in case of range II and the onset temperature of the main reaction is approximately 20°C lower. With very fine particles the reaction begins with full intensity at approximately 45°C and is nearly complete before melting of sulfur, as a consequence thermal effects of sulfur are not detectable.

Pellets revealed more differences in the intensity of DTA peaks than in the onset temperatures. With decreasing particle size (I → III) the reaction effect T5 increases, and the contribution of the following effects to the reaction enthalpy decreases. With pellets of fine powders the reaction peaks decrease in half-width and are better separated. Again the intense reaction before melting of sulfur is remarkable.

4.6. Influence of pretreatment and batch of educts

The influence of pretreatment on the reaction was investigated with sulfur as received (Merck, Fluka), recrystallised sulfur (Merck, Fluka), and sublimed sulfur (Fluka). The different sources of sulfur had no influence on the course of the reaction. Samples in powder and pellet form show variations in the DTA traces only in the case of sublimed sulfur. The onset temperatures of the effects P7 and T8 are shifted to higher temperatures by 50°C and the effects are more intense. The powders showed an additional effect at

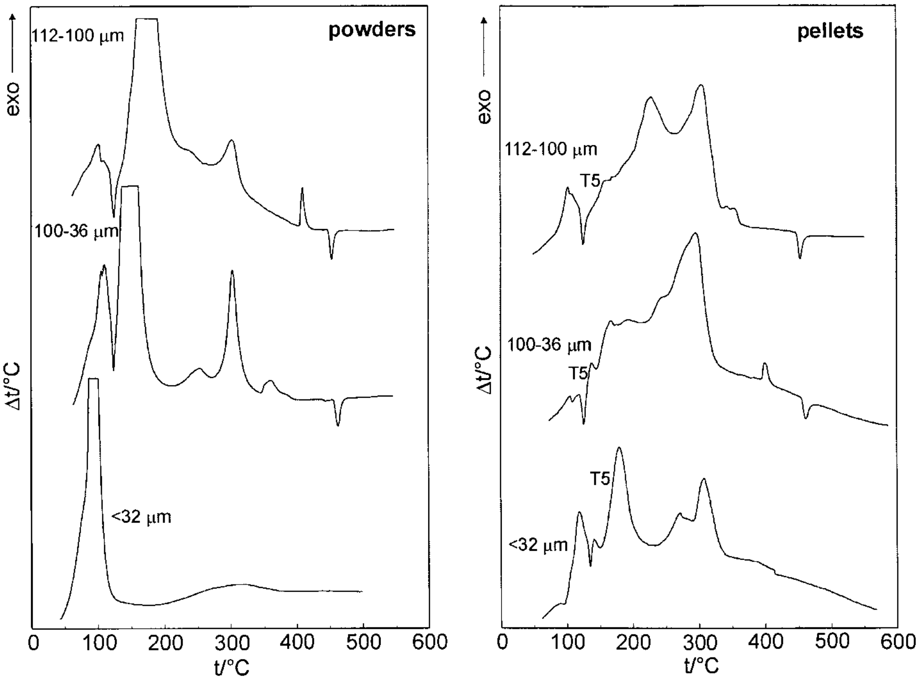

Fig. 10. DTA traces of reaction mixtures (2Cu+S) with different particle sizes of copper.

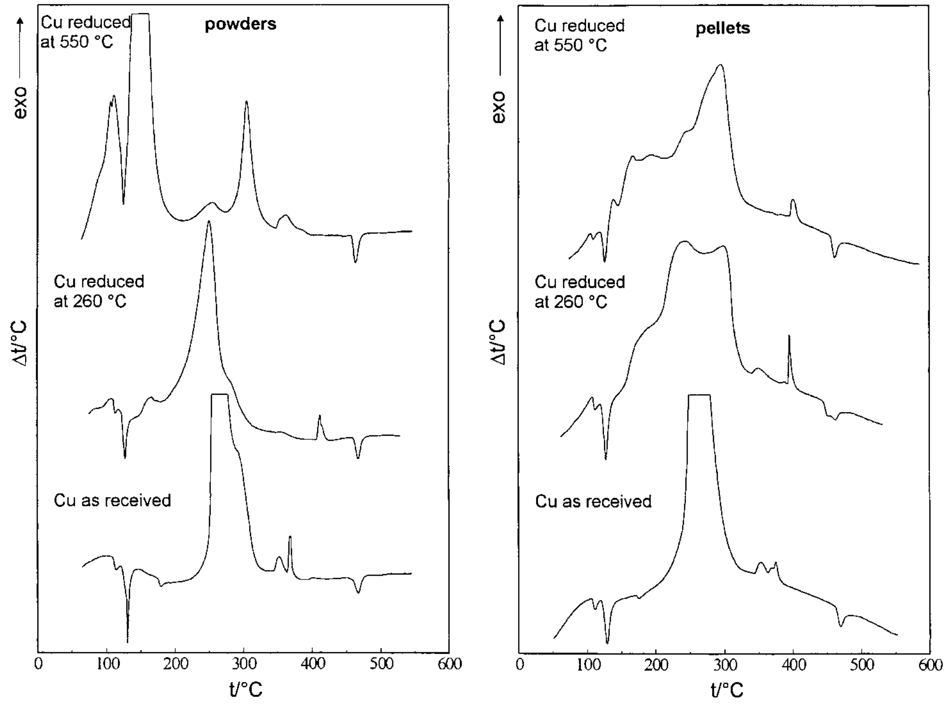

Fig. 11. DTA traces of reaction mixtures (2Cu+S) with copper powder, purified under different conditions.

187°C. Sublimation leads to an enrichment of volatile compounds in the sublimate, which seems to delay the start of some formation reactions during heating.

The influence of pretreatment of copper was investigated with copper (Hereaus) as received and copper reduced at 260°C with particle sizes in the range 36–100 μm. Copper reduced at 260°C contains still eutectic Cu_2O. Fig. 11 shows the respective DTA traces of powders and pellets. The differences in reaction behaviour are drastic, when compared with mixtures containing powders reduced at 550°C.

Copper as received does not turn grey during mortaring or pressing, because oxide layers prevent formation of CuS. DTA traces are nearly identical for powders and pellets. The small endothermic effect at approximately 170°C (polymerisation of sulfur) indicates that unreacted sulfur is present in larger amounts. The sulfide formation starts with a strong exothermic effect at 240°C in powders and 230°C in pellets and is then almost complete. Then some small exothermic effects follow between 350 and 400°C which are typical for untreated copper. They are probably caused by change from sulfur rich $Cu_{2-x}S$ to the two phase region $Cu_{2-x}S$+β-Cu_2S and the completion of the reaction by the formation of copper rich $Cu_{2-x}S$.

Since the reaction starts at temperatures where sufficient amounts of gaseous sulfur are available, all conditions which lead to the previously described different behaviour of powders and pellets can be discarded.

The reaction of Cu (reduced at 260°C) is intermediate between that of copper as received and copper powder, reduced at 550°C. It turns to grey on mortaring and pressing, but CuS is not observed in X-ray diffractograms. In the DTA traces the polymerisation effect of sulfur is missing because before and after melting sulfur is partly consumed. The main reaction is at least in powders shifted to higher temperatures but it starts still at low temperatures so that a difference between powders and pellets was found. These results confirm that reduction temperatures around 260°C are not sufficient.

The high reactivity of copper powders reduced at 550°C is not only due to removal of all oxides but also to a larger specific surface area resulting from embrittlement by hydrogen (Fig. 4f).

The same series of experiments was performed with copper powders with particle sizes <32 μm. The results revealed that the DTA traces are more similar to traces of larger particles, containing oxygen, than to those of oxygen free particles of the same size. Pretreatment is not important for copper powders with extremely large specific surface area (alfa, tinsel). These educts react completely in one strong exothermic effect without further reaction.

Despite the same pretreatment and same particle size range the reaction behaviour often differed, if copper powders of different manufacturers were used. We attribute this behaviour to differences in particle size distribution, particle shape, grain size, or oxygen contents of the powders. Fig. 4 shows the differences in particle shape.

4.7. Influence of ageing

A reaction between copper and sulfur during storage at room temperature was already observed by several authors [17,57,58], but not investigated in detail.

In a first series after each storage period the sample was mortared and a small part investigated in the form of powders and of pellets. The rest was stored again under the same conditions. Thus, total storage periods of 1, 2, 5, 10, 20 and 30 days were achieved. Fig. 12 shows the diffractograms, the DTA traces of pellets are given in Fig. 13.

In an inert atmosphere CuS was formed, its amount increased with time, after 30 days most sulfur was consumed. The mixtures darkened and the particle sizes increased, because the layers on the particles grew to the outside. DTA traces of samples in form of pellets aged in inert atmosphere are very similar to those of milled samples, because in both cases CuS is formed in the first stage. In Table 12 milling periods and storage times are listed, which give similar DTA curves.

Ageing in vacuum was different. In the first period CuS and Cu$_{1.8}$S were observed. After 2 days nearly the

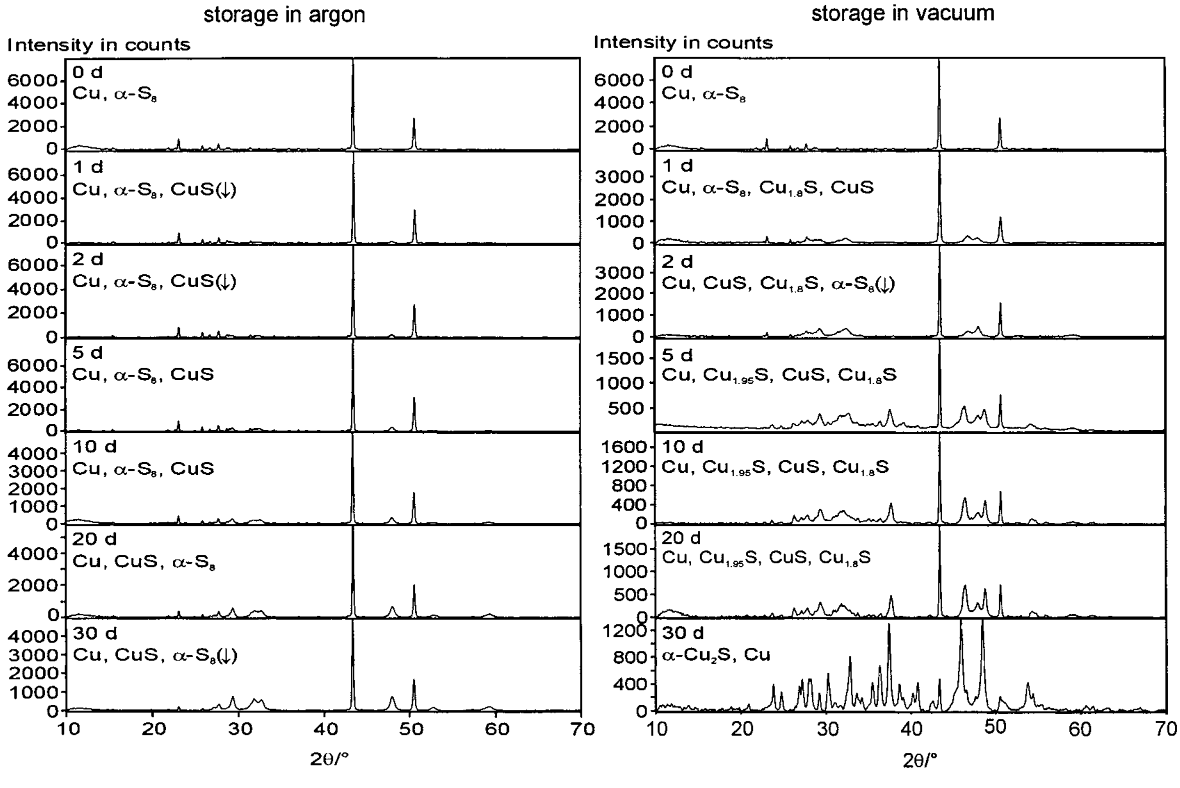

Fig. 12. XRD measurements following ageing experiments of mixtures (2Cu+S) depending on ageing time and ageing condition.

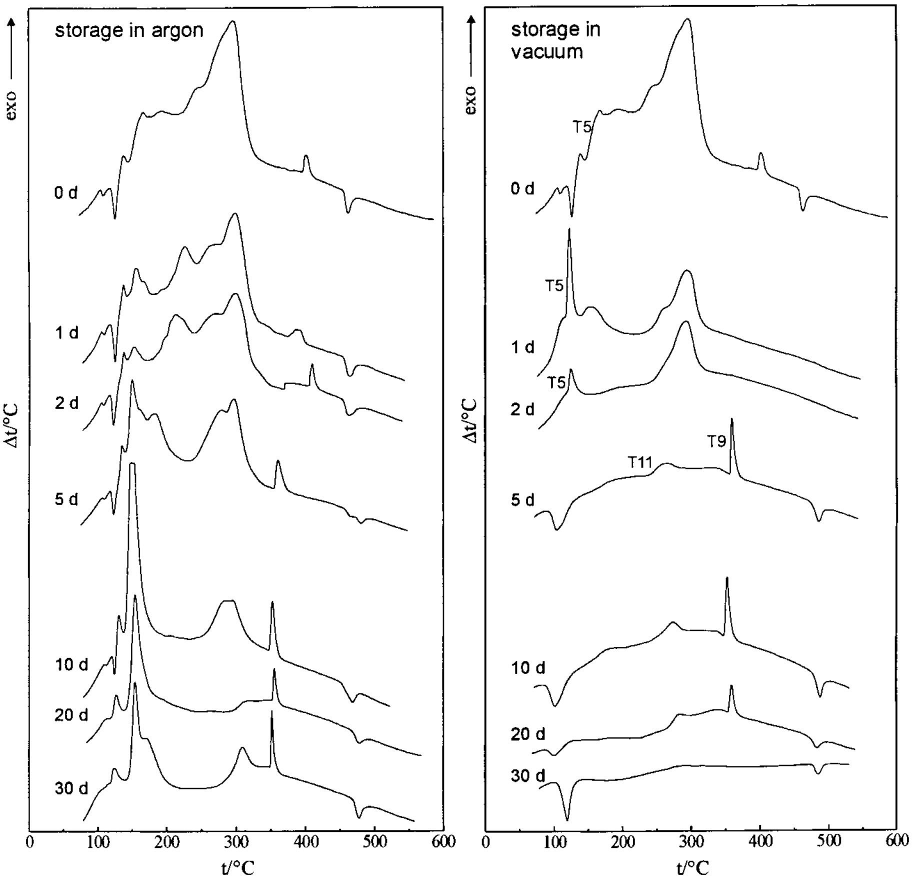

Fig. 13. DTA traces of pellets following ageing experiments of mixtures (2Cu+S) depending on ageing time and ageing condition.

same amount of sulfur was consumed as after 30 days in an inert atmosphere. The particle size increased considerably. After 5 days sulfur vanished in the diffractograms and the main product was $Cu_{1.95}S$. The following reactions up to 20 days storage time were slow, but after 30 days only α-Cu_2S and Cu were observed.

Table 12
Comparison of milling and storage times which lead to similar DTA traces

Milling time in planetary ball mill (min)	Storage time in argon (days)
1	1
5	10
10	30

DTA curves of pellets of these samples cannot be compared with those of other partly reacted mixtures (2Cu+S) because they contained other compounds than samples which were not aged before thermal analyses. After 1 or 2 days storage the formation of CuS is recognised by a sharp thermal effect (T5) before melting of sulfur approximately 30°C lower than in fresh samples. Phase transitions of sulfur are not detectable. DTA traces of samples aged in the range 5–20 days are very similar, because the reaction proceeds very slowly in this interval. All show the peritectoid decomposition of djurleite at 90°C, the formation of copper rich from copper poor $Cu_{2-x}S$ at 354°C (T9) and the small effect of the reaction $CuS+1-xCu \rightarrow Cu_{2-x}S$ ($x\approx0.2$) (T11). After 30 days the DTA trace is that of pure α-Cu_2S.

If powders were used for the DTA runs, the DTA curves of samples aged under inert gas compared with those of fresh mixtures showed that CuS forms in each case before (P2) and after melting of sulfur (P5). On the other hand the peaks (P6, P7) due to the formation of $Cu_{2-x}S$ are either weak or particularly not observable after short ageing. Powders stored in vacuum revealed that the main reaction takes place at lower temperatures together with melting of sulfur. The high temperature of the β-$Cu_2S \rightarrow Cu_{2-x}S$ ($x=0$) transformation at 485°C is surprising. After consumption of sulfur (5 days) powders and pellets have the same behaviour in DTA within the reproducibility.

The first reaction always occurs at lower temperatures in samples stored in vacuum and ground than in fresh samples. In both cases the surface is not covered by a product layer, but may be activated during storage. Such a honeycomb surface structure was observed by Lambertin and Colson [59] in the reaction of copper wires with gaseous sulfur.

The mixtures of the second series were stored for 2, 10, and 30 days in vacuum, respectively, and investigated as received or after mortaring. After 10 days roxbyite ($Cu_{1.75}S$) [60] besides other copper sulfides is formed and vanishes by mortaring. Anilite ($Cu_{1.75}S$) was not observed.

DTA curves of mortared mixtures and powders as received revealed significant differences only after 30 days. Mortared samples have a much larger first reaction effect, the next effects are comparable within the experimental reproducibility. Fig. 14 shows as example the DTA traces of mixtures stored 30 days in vacuum. This sample contained mainly copper rich sulfides. In both traces the first effect is due to the decomposition of djurleite. Only in the mortared sample the reaction of remaining Cu to copper rich $Cu_{2-x}S$ and the phase transformation β-Cu_2S to $Cu_{2-x}S$ ($x=0$) can be observed. The copper sulfides are removed by grinding from the surface of the copper particles so that the reaction can quickly occur. In samples which were not mortared this reaction takes place very slowly, because of the protecting copper sulfide layers. The phase transition cannot be observed, because the composition Cu_2S is reached above the phase transition temperature.

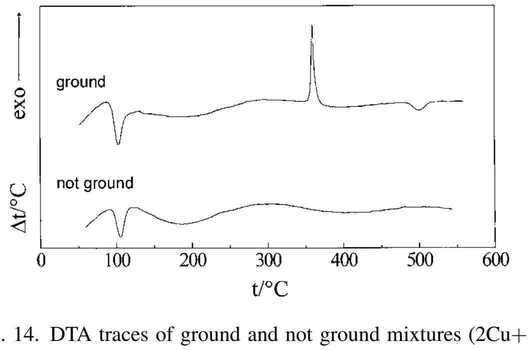

Fig. 14. DTA traces of ground and not ground mixtures (2Cu+S) after storage for 30 days in vacuum.

In the third series the educts were stored under vacuum for 2 days in the dark, in artificial light, and sunlight, respectively. In addition, educt mixtures in evacuated quartz ampoules and under argon were irradiated for 10 min with light evolved from hot quartz. All samples were investigated by powder diffractometry directly and after 28 days. The reaction is only influenced by the intense light effect of sealing of silica ampoules. After 10 min irradiation with intense light, in vacuum as well as under inert gas the amount of products was very small. In inert gas only CuS was formed, in vacuum CuS and $Cu_{1.8}S$. If the samples were stored for 28 days in inert gas, the sample irradiated under inert atmosphere showed only moderate progress of the reaction. The sample irradiated in vacuum contained CuS, $Cu_{1.8}S$, and $Cu_{1.95}S$. Apparently one short irradiation in vacuum accelerates the reaction at the beginning. The reason might be a dissociation of S_8 to the more reactive molecules S_6 and S_7.

In the fourth series a mixture with copper powder (Heraeus) as received was stored for 30 days. Due to the protecting oxygen surface layer this mixture did not react in inert gas, in vacuum traces of CuS were found.

All storage experiments revealed that metastable products are formed in lesser amounts than in milling experiments or in samples quenched from higher temperatures.

Ageing in inert atmosphere results in CuS and does not exceed this stage even after storage periods of several months. In vacuum influenced by intense light different intermediate products were observed from the beginning. The rate of reaction is very different under the same ageing conditions, however, with oxygen free copper powders reaction in vacuum is always faster than in inert gas.

In our opinion the reaction occurs between solids even in vacuum, and not between solid copper and gaseous sulfur. This is confirmed by the observation that sulfur at the walls of the ampoule reacts only when contact between this sulfur and Cu is achieved by shaking. The reaction of sulfur rich $Cu_{2-x}S$ to the final product is rapid.

4.8. Influence of the heating rate

The heating rate is a decisive factor for the reaction behaviour. DSC traces of pellets were taken with different heating rates. For comparison the heat flow was divided by the mass of the sample and the heating rate. Fig. 15 reveals that with a heating rate of 1.0 K/min the reaction is nearly finished below 100°C. Two main effects are observed with increasing heating rates. The peak temperatures increase, for the onset of the first main reaction from 122°C (2.5 K/min) to 181°C (40 K/min), similarly the end of the second peak shifts from 278 to 375°C. The amount of products formed after melting of sulfur increases from 11% with 2.5 K/min to 55% with 40 K/min. A possible explanation is the formation of a protecting sulfide layer before melting of sulfur at lower heating rates and the absence of this layer at higher heating rates. Contrary to the literature [1,25] the phase transition β-$Cu_2S \rightarrow Cu_{2-x}S$ (x=0) does not depend on the heating rate and is found at 449±1°C.

4.9. Self-propagating reactions

In self-propagating reactions the reaction front propagates after ignition through the educts with high speed.

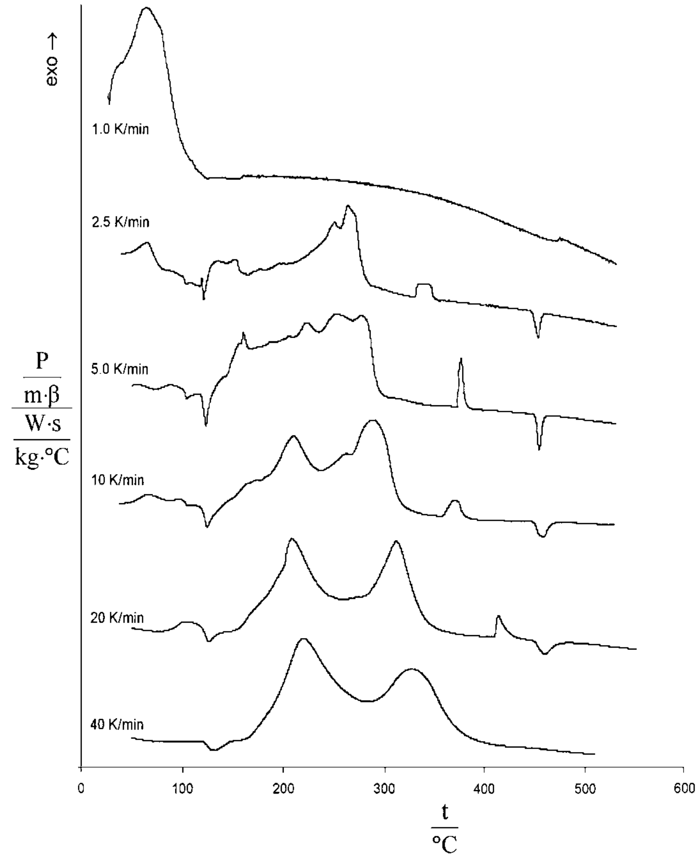

Fig. 15. DSC traces of pellets of mixtures (2Cu+S) measured at different heating rates.

Fischbeck observed the almost complete formation of Cu_2S during pressing pellets of reduced copper powders and sulfur [57]. In similar investigations it was shown that not pressure and time during pelletization, which determine the compound formation, but pressing temperature and surface of copper powders [11,61].

We found that at 30°C a self-propagating reaction starts in the press, indicated by a sudden decrease of pressure due to melting of sulfur. Reaction products are α-Cu_2S, $Cu_{1.95}S$, or $Cu_{1.8}S$, CuS, and amorphous sulfur, depending on the progress of the reaction.

Self-propagating reactions were also observed in DTA runs of powder samples which were free of oxygen and had a particle size <32 μm, revealed by a sudden increase of the sample temperature of about 65°C at approximately 110°C. After this effect no further peaks were detected. The same educt mixtures can be ignited with a hit in a mortar, or by punctual heating in an evacuated silica ampoule. Samples which were reacted in vacuum contained after the reaction α-Cu_2S, Cu, and $Cu_{1.96}S$, those reacted in air $Cu_{1.8}S$ [49,50], $Cu_{1.96}S$, Cu_2O, and $CuSO_4$. When these mixtures are pressed to pellets, no self propagating reactions were observed in thermal analyses, because a part of the reaction takes place already during pressing.

5. Conclusion

Several parameters, which influence the formation of Cu_2S from the elements, were investigated by thermal methods and XRD. The reaction behaviour is strongly influenced by the shape of the samples (powders or pellets), the heating rate, the particle size, pretreatment and source of copper. Copper sulfides can also be obtained by mechanical treatment in a ball mill or by ageing of powder mixtures in sealed quartz ampoules. Nearly all stable and some metastable copper sulfides are involved in the reaction pathways. In the beginning of the reaction sulfides with high sulfur content are formed. Successive products appear well separated during mechanochemical synthesis. Ageing in sealed quartz ampoules leads to simultaneous formation of intermediate products.

In a second paper the reaction of copper in form of foils and the role of diffusion will be described.

Acknowledgements

The authors express their gratitude to the 'Deutsche Forschungsgemeinschaft' and the 'Fonds der Chemie' for their support.

References

[1] D.J. Chakrabarti, D.E. Laughlin, Bull. Alloy Phase Diagrams 4 (1983) 254.

[2] R.J. Goble, Can. Mineral. 23 (1985) 61.

[3] W.G. Mumme, G.J. Sparrow, G.S. Walker, Mineral. Mag. 52 (1988) 323.

[4] M. Savelli, J. Bougnot, Top. Appl. Phys. 31 (1979) 213.

[5] M. Dachraoui, J. Vedel, Solar Cells 22 (1987) 187.

[6] V.N. Konev, V.N. Chebotin, S.A. Fomenkov, Inorg. Mater. 21 (1985) 166.

[7] V.M. Glazov, O.D. Shchelikov, A.S. Burkhanov, Inorg. Mater. 25 (1989) 633.

[8] W. Liang, M.-H. Whangbo, Solid State Commun. 85 (1993) 405.

[9] K. Fischbeck, O. Dorner, Z. Anorg. Chem. 182 (1929) 228.

[10] K. Fischbeck, O. Dorner, Z. Anorg. Chem. 184 (1929) 167.

[11] Gmelins Handbuch der Anorganischen Chemie, 8th Edition, Vol. Cu Main B1, Verlag Chemie, Weinheim, 1958, p. 470.

[12] P. Cavalotti, G. Salvago, Electrochim. Metall. 4 (1969) 181.

[13] P. Kalyanaraman, N. Vijayashree, A.G. Samuelson, Indian J. Chem., Sect. A: Inorg., Bio-inorg. Phys., Theor. Anal. Chem. 33A (1994) 281.

[14] M. Charbonnier, M. Murat, Therm. Anal., Proc. Int. Conf., 3rd Meeting 2 (1971) 547.

[15] G. Frenzel, Neues Jb. Miner. 93 (1959) 87.

[16] W. Jost, P. Kubaschewski, Z. Phys. Chem. 60 (1968) 69.

[17] G. Donnay, J.D.H. Donnay, G. Kullerud, Am. Mineral. 43 (1958) 228.

[18] S. Djurle, Acta Chem. Scand. 12 (1958) 1415.

[19] G.H. Moh, Carnegie Institute Washington Year Book 1962, 1963, p. 214.

[20] G.H. Moh, Mineral. Soc. Jpn. Spec. Pap. 1 (1971) 226.

[21] T. Ohtani, M. Motoki, K. Koh, K. Ohshima, Mater. Res. Bull. 30 (1995) 1495.

[22] D.J. Chakrabarti, D.E. Laughlin, in: T.B. Massalski (Ed.), Binary Alloys Phase Diagrams, 2nd Edition, Vol. 2, ASM International, USA, 1992, p. 1467.

[23] R.C. Sharma, Y.A. Chang, Metall. Trans. B 11B (1980) 575.

[24] R.W. Potter, Econ. Geol. 72 (1977) 1524.

[25] E.H. Roseboom Jr., Econ. Geol. 61 (1966) 641.

[26] C. Conde, C. Manolikas, D. Van Dyck, P. Delavignette, J. Van Landuyt, S. Amelinckx, Mater. Res. Bull. 13 (1978) 1055.

[27] I.S. Chaus, N.M. Kompanichenko, V.G. Andreichenko, Y.I. Gornikov, I.A. Sheka, Sov. Prog. Chem. 53 (1987) 6.

[28] S. Kashida, K. Yamamoto, J. Phys.: Condens. Matter 3 (1991) 6559.

[29] N. Morimoto, K. Koto, Y. Shimazaki, Am. Mineral. 54 (1969) 1256.

[30] F. Grønvold, S. Stølen, E.F. Westrum Jr., C.G. Galeas, J. Chem. Thermodyn. 19 (1987) 1305.

[31] S. Stølen, F. Grønvold, E.F. Westrum Jr., J. Chem. Thermodyn. 22 (1990) 1035.

[32] W. Smykatz-Kloss, K. Hausmann, J. Therm. Anal. 39 (1993) 1209.

[33] B. Gather, Thermodynamische Daten von Strukturen und Schmelzen. Ein Beitrag zum Verständnis der Schmelzen am Beispiel der Ia-Vb-VIb Systeme durch Messung und Rechnung der Phasenbeziehungen, Dissertation, Techn. Universität Clausthal, 1976.

[34] PDF-2 Database, International Centre for Diffraction Data, PA, USA, 1996.

[35] Inorganic Crystal Structure Database, Release 98/2, FIZ Karlsruhe, Gmelin Institute, 1998.

[36] Stoe & Cie GmbH, Version 3.01, 1996, Darmstadt.

[37] M. Nagamori, T.R. Ingraham, Metall. Trans. 2 (1971) 1501.

[38] H. Rajainmäki, A. Helenius, M. Kolehainen, JOM 45 (1993) 68.

[39] D. Röttges, H. Schliefer, J. Jacobsen, Metallurgy (Heidelberg) 52 (1998) 219.

[40] Gmelins Handbuch der Anorganischen Chemie, 8th Edition, Vol. Cu Main A2, Verlag Chemie, Weinheim, 1955, p. 684.

[41] A. Haas, J. Helmbrecht, U. Niemann, in: G. Brauer (Ed.), Handbuch der Präparativen Anorganischen Chemie, 3rd Edition, Vol. 2, Ferdinand Enke, Stuttgart, 1975, p. 971.

[42] W. Klement Jr., J. Polym. Sci. A-2 12 (1974) 815.

[43] G. Widmann, R. Riesen, Thermoanalyse: Anwendungen, Begriffe, Methoden, Hüthig, Heidelberg, 1984, p. 95.

[44] J. Chao, Hydrocarbon Process, Int. Ed. 59 (1980) 217.

[45] R. Steudel, H.-J. Mäusle, Chem. unserer Zeit 14 (1980) 73.

[46] R. Steudel, B. Holz, Z. Naturforsch. B 43b (1988) 581.

[47] PDF-2 Database, File 08-0247, International Centre for Diffraction Data, PA, USA, 1996.

[48] PDF-2 Database, File 06-0464, International Centre for Diffraction Data, PA, USA, 1996.

[49] PDF-2 Database, File 23-0962, International Centre for Diffraction Data, PA, USA, 1996.

[50] PDF-2 Database, File 41-0959, International Centre for Diffraction Data, PA, USA, 1996.

[51] Inorganic Crystal Structure Database, Release 98/2, File 100334, FIZ Karlsruhe, Gmelin Institute, 1998.

[52] PDF-2 Database, File 29-0578, International Centre for Diffraction Data, PA, USA, 1996.

[53] Inorganic Crystal Structure Database, Release 98/2, File 100333, FIZ Karlsruhe, Gmelin Institute, 1998.

[54] W.R. Cook Jr., Nat. Bur. Stan. Spec. Publ. 364, Solid state chemistry, in: Proceedings of the 5th Material Research Symposium, 1972, p. 703.

[55] Inorganic Crystal Structure Database, Release 98/2, Files 200986-200989, FIZ Karlsruhe, Gmelin Institute, 1998.

[56] PDF-2 Database, File 25-1047, International Centre for Diffraction Data, PA, USA, 1996.

[57] K. Fischbeck, Z. Anorg. Chem. 154 (1926) 261.

[58] M. Kazinets, L. Taidler, J. Cryst. Growth 83 (1987) 437.

[59] M. Lambertin, J.-C. Colson, Oxid. Metals 7 (1973) 163.

[60] PDF-2 Database, File 23-0958, International Centre for Diffraction Data, PA, USA, 1996.

[61] R. Mole, R. Hocart, Bull. Soc. Chim. France (1954) 977.